Ceramics International 42 (2016) 16242–16247

Contents lists available at ScienceDirect

Ceramics International

journal homepage: www.elsevier.com/locate/ceramint

Role of morphological characteristics on the conductive behavior of $LaNiO_3$ thin films

R.A.C. Amoresi [a], A.A. Felix [a], G.M.M.M. Lustosa [a,*], Gisane Gasparotto [a], A.Z. Simões [b], M.A. Zaghete [a]

[a] Interdisciplinary Laboratory of Electrochemistry and Ceramics, LIEC – Chemistry Institute, São Paulo State University – UNESP, Araraquara, SP, Brazil
[b] Faculty of Engineering of Guaratinguetá, São Paulo State University – UNESP, Guaratinguetá, SP, Brazil

ARTICLE INFO

Article history:
Received 15 April 2016
Received in revised form
21 July 2016
Accepted 22 July 2016
Available online 27 July 2016

Keywords:
A. Films
B. Surfaces
C. Electrical conductivity
E. Electrodes

ABSTRACT

$LaNiO_3$ (LNO) thin films were synthesized via the polymeric precursor method and sintered using conventional and microwave heating sources. The samples were characterized by structural morphological and electrical techniques. The crystalline structure was analyzed by X-ray diffraction and indicated rhombohedral perovskite phase in both films sintered using conventional and microwave heating. The films morphology was evaluated by scanning and transmission electron microscopy, and atomic force microscopy, and the results point out that microwave heating exerts direct influence on the morphological characteristics of LNO films contributing towards the change in the grain size distribution, porosity and roughness. Conductivity was also investigated through four-probe measurements, which pointed out a conductive and ohmic behavior of the LNO thin films prepared via the polymeric precursor method where a direct relationship was found between the morphological characteristics and the electrical properties of LNO film.

1. Introduction

Conductive oxides have been extensively studied as electrode layer in place of metallic electrodes in a vast array of applications, ranging from transparent electrodes for solar cells to bottom electrodes in ferroelectric memories [1–4]. These oxides are required to present several characteristics in order to be used as electrode, among such features include low resistivity, strong adhesion to the substrate, ohmic contact, chemical and thermal stability [3,4]. In recent years, researchers have focused their efforts on the study of conductive perovskite oxides obtained as thin films owing to the fact that they can act concomitantly as bottom conductive electrode and as template layer for the development of crystalline structure with preferred orientation [5–7]. For instance, the use of this class of oxides as bottom electrode in place of platinum electrodes in ferroelectric thin films based on perovskite oxides is found to lead to the enhancement of the strain effects at the film/electrode interface as a result of the similarity observed in the crystallographic structures, thereby contributing towards improving the hysteretic memory behavior [2,3,8–11]. Nonetheless, it is worth pointing out that the conductivity of these oxides is still lower at least by one or two order of magnitude compared to metal electrodes. Thus, studies aiming at finding new materials or optimizing the properties of the known ones are the main focus of researchers in an effort to effectively overcome the intrinsic shortcoming presented by both metallic and oxide electrodes.

Among other conductive perovskite oxides, several studies have shown that Lanthanum Nickelate $LaNiO_{3-\delta}$ (LNO) exhibits all the characteristics which render it suitable to be used as bottom electrode. This material has attracted great attention largely due to the excellent conductive behavior and the simple perovskite crystalline structure, making it very attractive to be used as bottom electrode in electronic devices based on ferroelectric and piezoelectric materials [4,5,7]. Admittedly, the relationship between the synthesis method and the electrical properties has, to date, not been fully established [7–14]. Sun et al. [13] have reported the preparation of LNO thin films on Si substrate by Pulsed Laser Deposition (PLD), showing a metallic behavior and resistivity of about $10^{-5}\,\Omega$ m. On the other hand, Li *et al.*[15] have shown that films prepared by chemical method on different substrates exhibit a resistivity in the range of 10^{-4} to $10^{-6}\,\Omega$ m. These studies have pointed out that conductive behavior in this material depends not only on the growth method but also on the intrinsic parameters of the deposition technique for the same method being used. Moreover, it is well known that the morphology characteristics, such as grain size and surface roughness of the films are directly related to the synthesis conditions and, consequently, connected to the electrical behavior of the material, which

* Corresponding author.
E-mail address: rafaelciola@yahoo.com.br (G.M.M.M. Lustosa).

http://dx.doi.org/10.1016/j.ceramint.2016.07.155
0272-8842/

is, in essence, not well defined in the literature for this material and still remains a topic of open discussion.

In light of these shortcomings, the main goal of this work was to investigate the structural, morphological and electrical properties of $LaNiO_3$ thin films prepared via the polymeric precursor method (PPM) using conventional and microwave heating sources aiming at establishing a relationship between the specific morphology characteristics, such as surface roughness, grain size, density and the electrical properties of this material.

2. Experimental details

2.1. Synthesis procedure

LNO films were prepared with the polymeric precursor method and the synthesis conditions used in this work were based on our previous works [16–18]. The polymeric solution was prepared at a molar ratio of metal: citric acid: ethylene glycol of 1:4:8. All reagents used had analytical purity. The precursor lanthanum solution was prepared through the dissolution of $La(NO_3)\cdot 6H_2O$ (Aldrich) in aqueous citric acid solution under stirring at room temperature. Afterwards, following homogenization, the temperature was increased to 90 °C for the formation of metal chelates. Similar procedure was employed towards obtaining the nickel precursor solution using $Ni(NO_3)\cdot 6H_2O$ (Vetec) as starting material. The polymer precursor solutions were subsequently stechiometrically mixed in order to obtain lanthanum nickelate solution at room temperature. After homogenization, the solution temperature was raised to 95 °C and ethylene glycol was added aiming at polymerizing the solution. The solution viscosity was adjusted to 20 cP by controlling the deionized water content using a viscometer (Brookfield, Model LV-DV3T).

The solution layers were deposited on Si (100) substrates by spin coating (Laurell, Model WS-650 MHz) operating at 5000 rpm for 30 s, followed by a pre-treatment at 120 °C for 20 min to remove solvent excess. This process was repeated 6 times. The films were then annealed at 400 °C for 1 h using a heating rate of 3 °C/min in conventional furnace to remove organic material. After that, the thin films were annealed at 700 °C using a heating rate of 10 °C/min at different times in conventional (LNO-A) and microwave (LNO-B) furnaces to obtain the crystalline phase, shown in scheme of the Fig. 1. The microwave furnace was operated by means of a PID controller at 770 W and frequency of 2.45 GHz using a rounded SiC as heating susceptor.

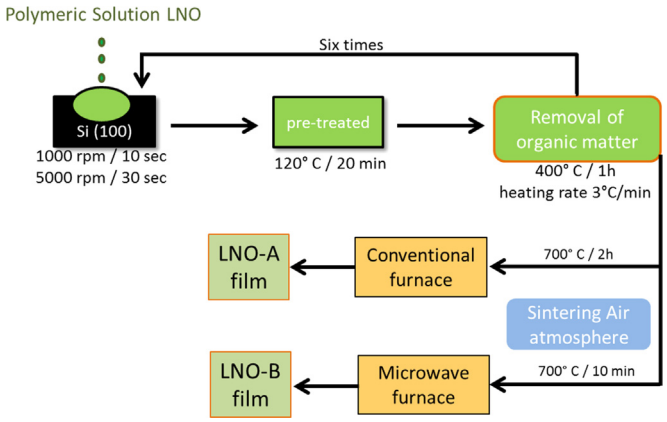

Fig. 1. Illustrative scheme of the synthesis procedure of the thin films.

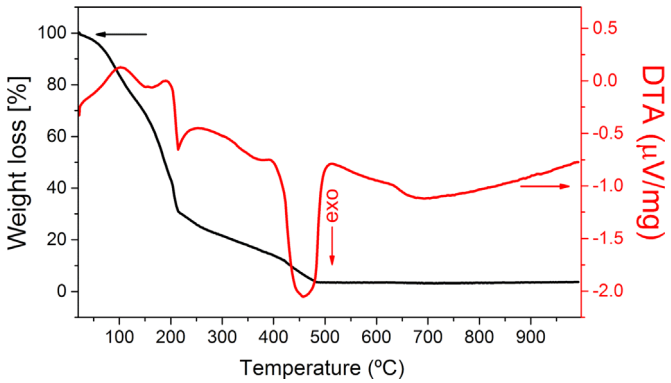

Fig. 2. Thermogravimetric analysis of LNO polymeric solution.

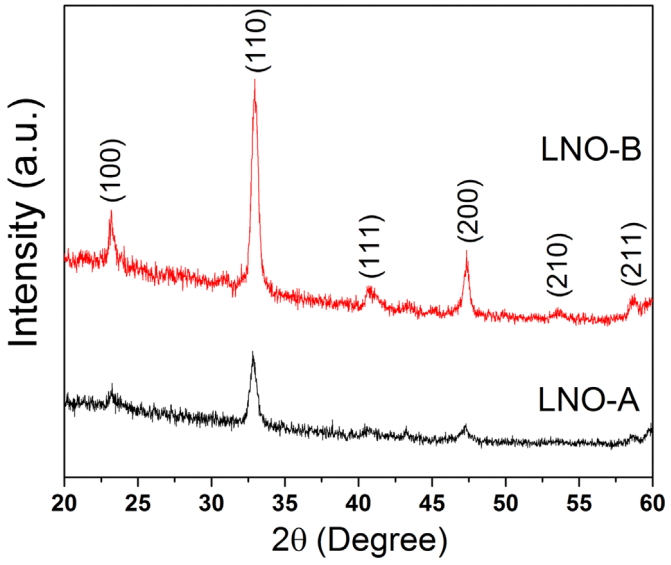

Fig. 3. XRD patterns of LNO films sintered via (a) conventional (LNO-A) and (b) microwave (LNO-B) heating sources.

2.2. Characterizations

Thermogravimetric analysis (TG) and differential thermal analysis (DTA) (Netsch, Model STA 409) were used to determine the decomposition temperature of the LNO polymeric solution and average phase crystallization temperature. These analyses were performed by means of a standard alpha alumina (α-Al_2O_3) sample holder using a heating rate of 10 °C/min in atmospheric air. Thin films phase analysis was performed through X-ray diffraction (XRD; Rigaku, Model Rint 2000) at room temperature using Cu Kα radiation. The XRD patterns of the samples were identified based on the cards of the *Joint Committee on Powder Diffraction Standards (JCPDS)*.

Morphology and thickness of the samples were analyzed using a field emission gun scanning electron microscope (FEG-SEM; JEOL, Model 7500 F) and a transmission electron microscopy (TEM; Philips CM-20). The surface morphology of the thin films was characterized by atomic force microscopy (AFM; Digital Instruments, Model NanoScope IIIa) using tapping mode. The electrical measurements of the LNO films were carried out using a resistivity measurement system (Signatone, Model Pro-4) operating on four probe mode connected to an established voltage source meter (Keithley, Model 2400).

3. Results and discussion

TG/DTA analysis of the polymeric solution is shown in Fig. 2

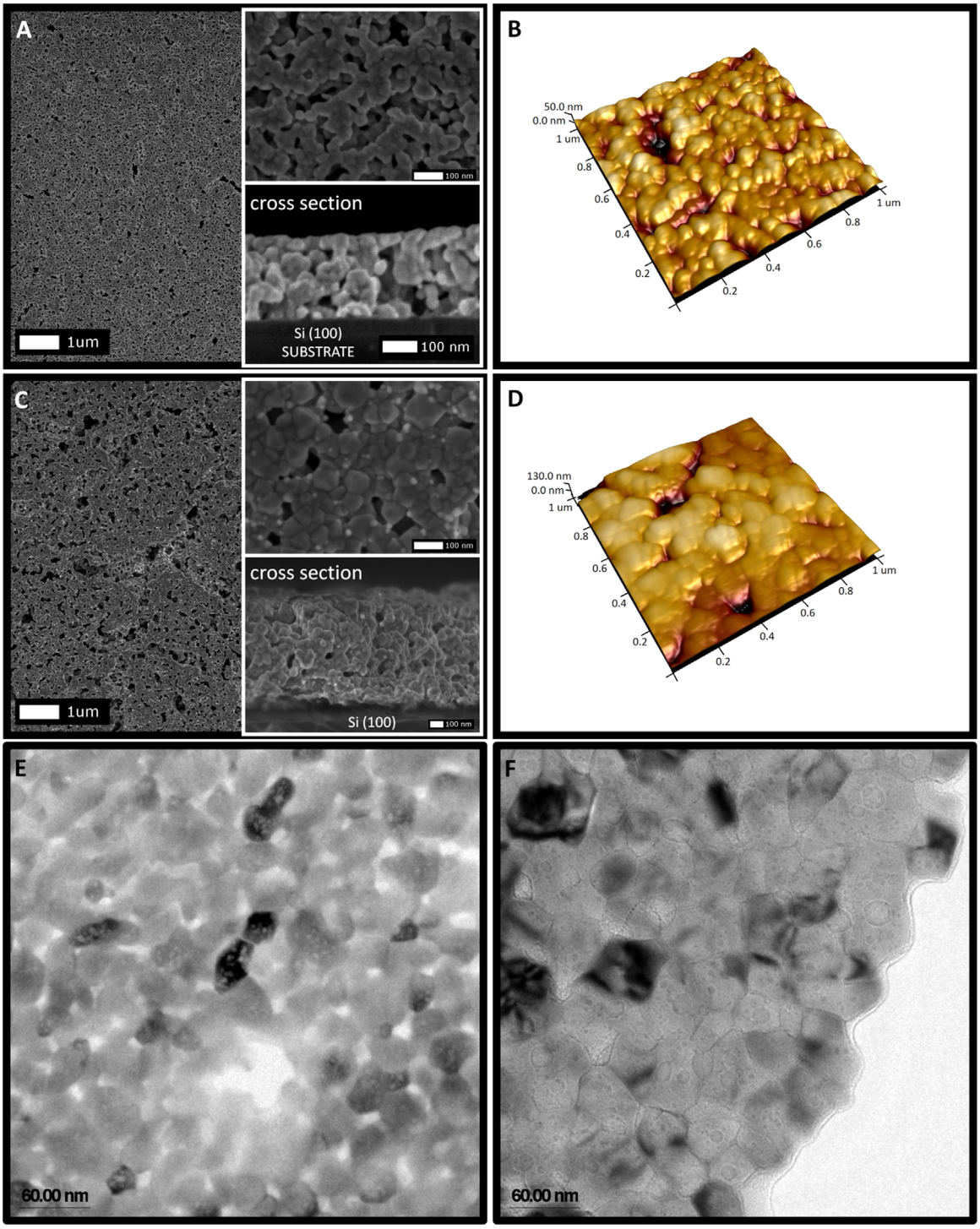

Fig. 4. SEM, AFM and TEM images of LNO films sintered by (a, b, e) conventional (LNO-A) and (c, d, f) microwave (LNO-B) heating sources.

Table 1
Thickness, surface roughness, average grain size and sheet resistivity of the LNO films.

Film	Thickness (nm)	Roughness (nm)	Average Grain size (nm)	Sheet Resistivity (μΩ m)
LNO (A)	230	12	53	117
LNO (B)	765	66	65[a]	256

[a] Based on statistical distribution.

which indicates three regions of weight loss related to different chemical reactions. The first region up to 150 °C showed a weight loss of about 15% related to the evaporation of water resulting from the polyesterification reaction [19]. The second region between 150 °C and 210 °C is associated with the elimination of volatile residues owing to the beginning of polyester decomposition with a weight loss of about 50%. The last 25% of weight loss between 210 °C and 480 °C is attributed to the final decomposition of organic compounds, as reported in the literature [19], while no weight loss is observed above this temperature indicating the complete decomposition of the polymer. The exothermic peak

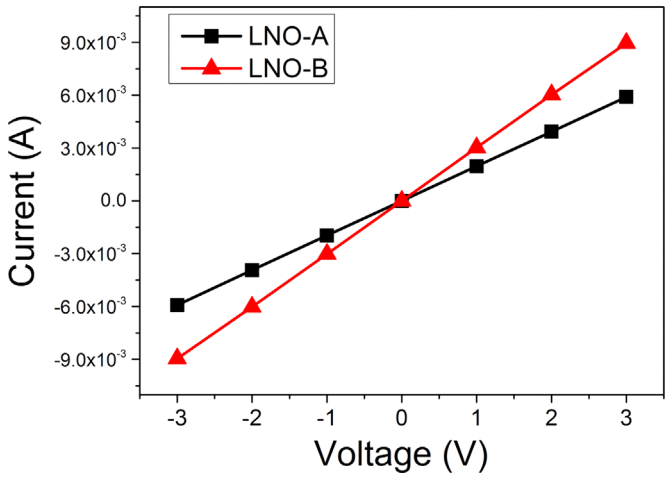

Fig. 5. Four-probe current *vs.* voltage measurements of LNO thin films.

observed in the range of 400–500 °C can be related to the combustion of organic compounds while the endothermic peak at 630 °C is attributed to the $LaNiO_3$ phase crystallization [10].

Based on TG/DTA results, the LNO films were sintered at 700° C using two different heating sources and analyzed by XRD, as shown in Fig. 3. In both films, the peaks were indexed as the rhombohedral phase (#34-1028) with space group $R-3m$. The XRD pattern showed that the LNO films were free of secondary phases and the relative intensities of the peaks indicated the formation of polycrystalline LNO without preferential orientation [20]. Furthermore, the phase crystallization time is found to decrease from 2 h with conventional heating to 10 min with microwave heating, indicating that the microwave induces the LNO phase crystallization at shorter time, in accordance with the results reported in the literature for perovskite-type oxides [21].

Fig. 4 shows the morphological analysis of the LNO thin films prepared via different heating sources. Surface SEM images of the film sintered via conventional heating (Fig. 4a) presents a smooth surface and a homogeneous grain size distribution, with average grain size of 50 nm, and low porosity, while the film sintered by microwave heating (Fig. 4c) exhibits an irregular surface with a non-homogeneous grain size distribution, composed of larger and small grains with average grain size of 90 nm and 25 nm, respectively, and high porosity which is a typical morphology exhibited by films sintered by the microwave heating method [22]. These results were corroborated by TEM analysis (see Fig. 4e–f) which indicates a similar grain size distribution observed through SEM analysis, as well as 3D-AFM images show that the film sintered by microwave heating exhibiting a surface roughness of more than 5-fold larger (see Table 1) compared to the film sintered via the conventional method, as shown in Fig. 4b–d. All films exhibit good adhesion on the silicon substrate for both heating methods, as shown through the SEM cross section images (see inset Fig. 4a-c). In addition, films with thickness less than 500 nm were expected by the synthesis procedure used in this work. However, the average thickness around 230 nm and 760 nm observed for conventional and microwave heating methods, respectively, indicates that microwave heating leads to a lower densification of the films compared to conventional heating.

The heating method adopted during the sintering process tends to exert a direct influence on mass transport in solid materials [23,24]. Based on these assumptions, we hypothesize that the microwave heating method induced a bimodal grain size distribution and low densification of the LNO films as a result of the rapid phase crystallization, in which the microwaves transfer energy directly to the molecules of the material leading to a significant decline in the phase crystallization time. As a result is taken to a rapid nucleation in the initial stage of the densification process allowing a fast mass transport across the grain boundaries. This process leads to an abnormal grain growth of LNO phase and, consequently, a morphology with high surface roughness and porosity due to the short time of the sintering process [25,26]. In summary, it is evident from our findings that microwave heating affects the morphology evolution of LNO phase, though it is not fully clear whether the densification process follows the classical mass transport mechanisms.

A linear relationship between the applied voltage and the current for both LNO films can be observed in Fig. 5, indicating a conductive and ohmic behavior in these films. The sheet resistivity of both films was about $10^{-4}\,\Omega$ cm though the microwave heated film exhibited a sheet resistivity more than 2-fold larger compared to that of the conventionally heated one, as shown in Table 1. Our results are consistent with the values reported in the literature for LNO bottom electrodes obtained as polycrystalline or epitaxial films [9,27]. Furthermore, these results indicate that the electrical characteristics are directly related to the morphological characteristics once the only perceptible difference between the films lies in the sintering process involving the use of different heating sources that tend to lead to different morphological characteristics [21]. The film sintered via conventional heating presents an

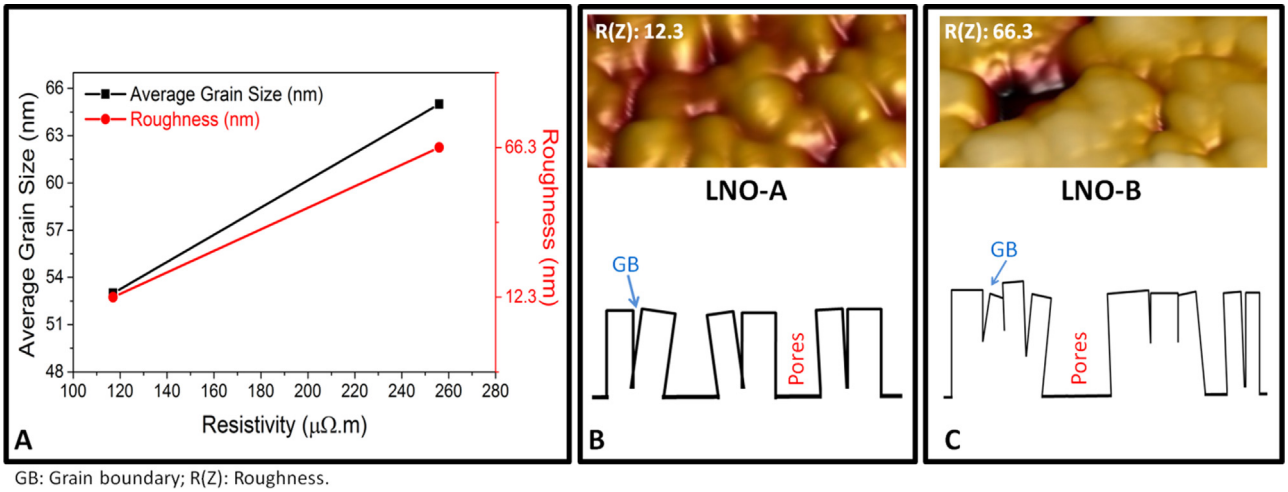

GB: Grain boundary; R(Z): Roughness.

Fig. 6. (a) Average grain size and roughness versus resistivity of LNO films. Comparison of the schematic conduction model and surface morphology of LNO films sintered by (b) conventional (LNO-A) and (c) microwave (LNO-B) heating sources.

ordered grain distribution, low roughness and porosity with a lower sheet resistance compared to the one sintered by microwave furnace which exhibits a disordered grain distribution, high roughness and porosity. Fig. 6a shows a relationship between the grain size, surface roughness and resistivity of the films where a decline in sheet resistivity can be seen given a reduction in grain size and surface roughness.

Recently, a theoretical model has proposed a relationship between the morphological characteristics of metallic polycrystalline samples with its electrical behavior [28]. This model is based on the scattering of electrons by grain boundaries and pores which affect the mean free path electron and, consequently, the material conductivity. In turn, the conduction of oxide materials is related to electrostatic potential barriers formed at grain boundary regions because of the formation of high angle line defects between the grains crystalized in different crystallographic orientations [29]. These potential barriers, known as back-to-back Schottky barriers, act by blocking/controlling the electron flow across the grain boundaries, and therefore the material conductivity [30]. Thus, it is expected that both mechanisms may coexist in LNO polycrystalline samples given that it is an oxide material with a metallic behavior, i.e., these mechanisms may work concomitantly affecting the LNO conductivity.

Based on these assumptions, we believe that the bimodal grain size distribution increases the number of grain boundaries, resulting in an increase in the number of potential barriers in the microwave heated film which leads to a decline in the film conductivity. Moreover, the high concentration of pores along with the high surface roughness these films can to act by scattering or trapping the electrons, increasing the mean free electron path and contributing to increase resistivity of the film sintered by microwave. A reverse behavior is observed when it comes to the films sintered via conventional heating. A schematic relationship between the grain size and roughness with the formation of potential barriers as well as the mean free electron path in LNO-A and LNO-B films respectively, are shown in Fig. 6b–c. Therefore, the relationship between the electrical parameters (number of potential barriers and mean free electron path) and the morphological characteristics (grain size distribution, surface roughness, porosity) provide a physical phenomenological explanation for the conduction behavior observed in LNO thin films sintered by microwave and conventional heating. However, prior to ascertaining whether this relationship is the main mechanism controlling the conduction characteristics of LNO thin film, additional studies, which are already in progress, must be performed in order to deconvolute the various contributions to the overall LNO conductivity while proposing a mathematical theory to support this relationship.

4. Conclusions

LNO thin films were synthesized via the polymeric precursor method on Si substrates using different heating mechanisms. Our results essentially show that the heating method exerts no influence on the structural properties through the XRD analysis, which is, in effect, a clear indication that the films are composed of polycrystalline LNO single-phase. However, it was found that the heating mechanism has a direct influence on the morphological characteristics leading to different nucleation and growth grain and, consequently, to different morphologies and density of the films. Current *vs.* voltage measurements were performed showing that all the films investigated presented good conductive behavior yet with different resistivity depending on the morphological characteristics of the films. These morphological parameters are controlled by the heating method during the sintering process and are intimately associated with the electronic conduction of this perovskite oxide. Reasons attributed to this behavior were proposed, where the formation of potential barriers and the mean free electron path were identified as the main mechanisms responsible for the control of conductivity in LNO thin films. Certainly, this study will contribute to the development of future applications of these bottom electrodes in various types of electronic devices.

Acknowledgments

The authors would like to warmly express their gratitude and indebtedness to the São Paulo Research Foundation (FAPESP) (Grant CEPID/CDMF-FAPESP: 2013/07296-2) and the National Council for Scientific and Technological Development (CNPq) (Grant: 165902/2015-9) for the financial support granted in the course of this research. We are also grateful to the LMA-IQ for providing the FEG-SEM facilities.

References

[1] S. Boscarino, I. Crupi, S. Mirabella, F. Simone, A. Terrasi, TCO/Ag/TCO transparente electrodes for solar cells application, Appl. Phys. A 116 (2014) 1287–1291.
[2] A.Z. Simões, E.C. Aguiar, C.S. Riccardi, E. Longo, J.A. Varela, Fatigue and retention properties of $Bi_{3.25}La_{0.75}Ti_3O_{12}$ films using $LaNiO_3$ bottom electrodes, Mater. Charact. 60 (2009) 353–356.
[3] S.J. Chiu, Y.T. Liu, G.P. Yu, H.Y. Lee, J.H. Huang, Enhancement of epitaxial $LaNiO_3$ electrode on the ferroelectric property of La-doped $BiFeO_3/SrTiO_3$ artificial superlattice structure by rf sputtering, J. Cryst. Growth 368 (2013) 1–5.
[4] I. Shturman, G.E. Shter, A. Etin, G.S. Grader, Effect of $LaNiO_3$ electrodes and lead oxide excess on chemical solution deposition derived $Pb(Zr_x,Ti_{1-x})O_3$ film, Thin Solid Films 517 (2009) 2767–2774.
[5] K.P. Rajeev, G.V. Shivashankar, A.K. Raychaudhuri, Low-temperature electronic properties of a normal conducting perovkite oxide ($LaNiO_3$), Solid State Commun. 79 (1991) 591–595.
[6] J.B. Goodenough, J.S. Zhou, Orbital ordering in orthorhomibic perovskites, J. Mater. Chem. 17 (2007) 2394–2405.
[7] D.S.L. Pontes, A.J. Chiquito, F.M. Pontes, E. Longo, Structural, dielectric, ferroelectric and optical properties of PBCT, PBST and PCST complex thin films on $LaNiO_3$ metallic conductive oxide layer coated Si substrates by the CSD technique, J. Alloy. Compd. 609 (2014) 33–39.
[8] E.C. Aguiar, M.A. Ramirez, J.A. Cortez, L.S. Rocha, E. Borsari, A.Z. Simões, Magnetoelectric coupling of $LaFeO_3/BiFeO_3$ heterostructures, Ceram. Int. 41 (2015) 13126–13134.
[9] X.J. Meng, J.G. Cheng, H.J. Sun, H.J. Ye, S.L. Guo, J.H. Chu, Growth of (100)-oriented $LaNiO_3$ thin films directly on Si substrates by a simple metalorganic decomposition technique for the highly oriented PZT thin films, J. Cryst. Growth 220 (2000) 100–104.
[10] D. Aman, T. Zaki, S. Mikhail, S.A. Selim, Synthesis of a perovkite $LaNiO_3$ nanocatalyst at a low temperature using single reverse microemulsion, Catal. Today 164 (2011) 209–213.
[11] H.T. Vu, M.D. Nguyen, E. Houwman, M. Boota, M. Dekkers, H.N. Vu, G. Rijnders, Ferroelectric and piezoelectric responses of (110) and (001)-oriented epitaxial $Pb(Zr_{0.52}Ti_{0.48})O_3$ thin films on all-oxide layers buffered silicon, Mater. Res. Bull. 72 (2015) 160–167.
[12] X.D. Zhang, X.J. Meng, J.L. Sun, T. Lin, J.H. Ma, J.H. Chu, D.Y. Kwon, C.W. Kim, B. G. Kim, Preparation of $LaNiO_3$ thin films with very low room-temperature electrical resistivity by room temperature sputtering and high oxygen-pressure processing, Thin Solid Films 516 (2008) 919–924.
[13] L. Sun, T. Yu, Y.-F. Chen, J. Zhou, N. Ming, Conductive $LaNiO_3$ electrode grown by pulsed laser ablation on Si substrate, J. Mater. Res. 12 (1997) 931–935.
[14] S. Sergeenkov, L. Cichetto Jr, M. Zampieri, E. Longo, F.M. Araújo-Moreira, Scaling like behavior of resistivity observed in $LaNiO_3$ thin films grown on $SrTiO_3$ substrate by pulsed laser deposition, J. Phys. Condens. Matter 27 (2015) 485307.
[15] A.-D. Li, C.-Z. Ge, D. Wu, P. Lu, Y.-Q. Zuo, S.-Y. Yang, N.-B. Ming, Conductive metallic $LaNiO_3$ films from metallo-organic precursors, Thin Solid Films 298 (1997) 165–169.
[16] A.A. Felix, J.L.M. Rupp, J.A. Varela, M.O. Orlandi, Multi-functional properties of $CaCu_3Ti_4O_{12}$ thin films, J. Appl. Phys. 112 (2012) 054512.
[17] M.G.A. Ranieri, M. Cilense, E.C. Aguiar, C.C. Silva, A.Z. Simões, E. Longo, Electrical behavior of chemically grown lanthanum ferrite thin films, Ceram. Int. 42 (2016) 2234–2240.
[18] M.G. Ranieri, R.A.C. Amoresi, M.A. Ramirez, J.A. Cortes, L.S.R. Rocha, C.C. Silva, A.Z. Simões, Magnetoelectricity at room temperature in the $LaFeO_3/BiFeO_3$

heterostructures, J. Mater. Sci. Mater. Electron. (2016), http://dx.doi.org/10.1007/s10854-016-4972-9.
[19] E.C. Paris, E.R. Leite, E. Longo, J.A. Varela, Synthesis of $PbTiO_3$ by use of polymeric precursors, Mater. Lett. 37 (1998) 1–5.
[20] X. Yang, J. Cheng, S. Yu, F. Chen, Z. Meng, Effect of $LaNiO_3$ sol concentration on the structure and dielectric properties of $Pb(Zr_{0.53}Ti_{0.47})O_3$ thin films grown on $LaNiO_3$-coated Si substrates, J. Cryst. Growth 310 (2008) 3466–3469.
[21] S.M. Zanetti, J.S. Vasconcelos, N.S.L.S. Vasconcelos, E.R. Leite, E. Longo, J. A. Varela, Low temperature crystallization of $SrBi_2TaO_9$ thin films using microwave oven, Thin Solid Films 466 (2004) 62–68.
[22] A.Z. Simões, C.S. Riccardi, M.A. Ramírez, L.S. Cavalcante, E. Longo, J.A. Varela, Synthesis and characterization of $CaBi_4Ti_4O_{15}$ thin films annealed by microwave and conventional furnaces, Solid State Sci. 9 (2007) 756–760.
[23] V. Mamedov, Spark plasma sintering as advanced PM sintering method, J. Powder Metall. 45 (2002) 322–328.
[24] E.T. Thostenson, T.W. Chou, Microwave processing: fundamental and applications, Compos. A Appl. Sci. Manuf. 30 (1999) 1055–1071.
[25] S. Balaji, D. Mutharasu, N.S. Sbramanian, K. Ramanathan, A review on microwave synthesis of electrode materials for lithium-ion batteries, Ionics 15 (2009) 765–777.
[26] J.N. Hart, Y.B. Cheng, D. Menzies, G.P. Simon, L. Spiccia, A comparison of microwave and conventional heat treatment of nanocrystalline titanium dioxide, Sol. Energy Mater. Sol. Cells 91 (2007) 6–16.
[27] V.T. Hien, N.D. Minh, V.N. Hung, Synthesis and characterizations of sol-gel-derived $LaNiO_3$ thin-film electrodes on Si substrates, Int. J. Nanotechnol. 12 (2015) 496–504.
[28] A.F. Mayadas, M. Shatzkes, Electrical-resistivity model for polycrystalline films: the case of arbitrary reflection at external surfaces, Phys. Rev. B 1 (1970) 1382–1389.
[29] B.U. Kingery, Introduction to Ceramics, 2nd ed., Wiley, New York, 1976.
[30] S.A. Pianaro, P.R. Bueno, P. Olivi, E. Longo, J.A. Varela, Electrical properties of the SnO_2-based varistor, J. Mater. Sci. 9 (1998) 159–162.